JOURNAL OF PROPULSION AND POWER
Vol. 11, No. 2, March–April 1995

Mixing and Chemical Kinetics Interactions in a Mach 2 Reacting Flow

Corin Segal,* James C. McDaniel,† Robert B. Whitehurst,‡ and Roland H. Krauss§
University of Virginia, Charlottesville, Virginia 22901

An experimental study of transverse hydrogen injection and combustion behind a rearward-facing step into a Mach 2 airflow was conducted in an electrically heated (not vitiated), continuous-flow facility to evaluate the effects of initial conditions (temperature, pressure, and equivalence ratio), and analyze the interactions between mixing and combustion in supersonic, reacting flows. Neither mixing nor reaction rates dominate in this particular regime, thus the use of initial conditions to scale fuel mixing (i.e., dynamic pressure ratio) has to be modified by a descriptor that includes the effects of combustion on the flow conditions at the fuel injection station. Combustor inlet static pressure was varied from 0.25 to 0.5 atm, and total temperature from 300 to 850 K. Injector configurations include both single and staged injection with injectors of 1 and 1.5 mm diam, transverse to the airflow, behind a 5-mm rearward-facing step. Images of visible flame emission distribution at several temperatures correlated with pressure and temperature measurements are used to describe the coupling between fluid dynamics and chemical kinetics, discussed in terms of a characteristic global Damköhler number (ratio of chemical reaction rate to turbulent mixing rate). A proposed modification to mixing scaling with dynamic pressure ratio in the presence of heat release effects is presented.

Nomenclature

H = step height
$\dot{m}_a$ = air flow rate
$\dot{m}_f$ = fuel flow rate
P_s = static pressure
P_0 = freestream static pressure
Q_r = dynamic pressure ratio
Q_w = wall heat transfer
η_c = combustion efficiency
η_m = mixing efficiency
τ_f = fluid residence time
τ_{ig} = ignition delay time
τ_r = reaction time
ϕ_r = reacted equivalence ratio
ϕ_t = total injected equivalence ratio

Introduction

EXPERIMENTAL and numerical investigations of the mixing and combustion in supersonic combustion flowfields are conducted to investigate the effects and the interaction between turbulent, compressible mixing, and heat release. In nonreacting shear layers, it has been well quantified that increased compressibility reduces the shear layer growth.[1,2] The convective Mach number, used as a compressibility parameter, indicates a decrease in turbulence and shear layer growth with increased compressibility.[3] This compressibility effect was also identified in chemically reacting flows.[4] In low-speed, turbulent shear layers, it has been indicated that the heat released by exothermic reactions causes a reduction in the growth rate.[5]

In transverse flows, mixing and heat release effects are further complicated by the complexity of the three-dimensional flow structure and the presence of shock waves. Numerous experiments[6–8] studied parametric effects of geometry and initial conditions and defined parameters that describe mixing and combustion efficiency. Usually defined as a certain degree of consumption of the fuel, these parameters provide a comparison between the set of conditions and design trends. In most cases, mixing efficiency is calculated with empirical relations, obtained in nonreacting flows, while combustion efficiency is evaluated as a degree of completion of chemical reactions, thus decoupling mixing from the effects of heat release. The strong three dimensionality of such an environment causes the flow to become either mixing- or kinetics-limited (Damköhler number has a broad variation around unity depending both on the spatial location and the species under investigation), and a strong interaction exists between the fluid dynamics and chemical kinetics, and the two effects cannot be uncoupled.

In the following sections an experimental investigation of the combined effects of mixing and combustion in a supersonic flow with transverse injection and combustion of hydrogen is presented. The coupling between mixing and combustion is described for a characteristic Damköhler number, representing the formation of water, estimated to be $\mathcal{O}(1)$.

In transverse or oblique injection the degree of jet penetration, as a measure of mixing, is often scaled with the dynamic pressure ratio of the jet to the freestream. In reacting flows, the effects of chemical reactions modify the near-field parameters in the vicinity of the jet and, as a result, the parameters responsible for mixing (and combustion), are changed. This suggests that the dynamic pressure ratio, as defined, needs to be modified to include the effects of heat release on mixing. A proposed modification of this parameter is suggested in a following section.

Vitiation often occurs in chemically heated facilities, in the form of water vapor or hydrocarbons reaction products, depending on the fuel used to heat the air. It has been shown[9] that in the low inlet total temperature regime (i.e., stagnation temperatures below 1000 K), vitiation increases the ignition delay time by as much as an order of magnitude, resulting in substantial lower reaction rates than expected in a full-scale scramjet in flight. This effect is due primarily to the third-

Received Oct. 2, 1993; revision received July 11, 1994; accepted for publication July 29, 1994.

*Research Assistant, Department of Mechanical, Aerospace and Nuclear Engineering; currently Assistant Professor, University of Florida, Gainesville, FL 32611. Senior Member AIAA.

†Associate Professor, Department of Mechanical, Aerospace and Nuclear Engineering. Member AIAA.

‡Research Scientist, Department of Mechanical, Aerospace and Nuclear Engineering. Member AIAA.

§Research Associate Professor, Department of Mechanical, Aerospace and Nuclear Engineering. Member AIAA.

body efficiency of the H_2O in the HO_2 formation reaction, which depletes the pool of free H radicals. The experiments reported herein cover the low-temperature, low-equivalence ratio range of a constant area scramjet model in a nonvitiating, resistively heated facility, thus unaffected by the vitiation effects mentioned above.

The tests presented below were conducted in a generic model with transverse hydrogen injection at sonic conditions behind a rearward-facing step, into a Mach 2 airstream. One- or two-staged injectors were used with exit orifice diameters of 1, 1.5, and 2 mm. The air stagnation temperatures were maintained around or below 850 K and the static pressure at the combustor entrance ranged from 0.25 to 0.5 atm.

Apparatus

Facility

A high-stagnation-temperature, clean-air, continuous-flow facility was designed and built for supersonic hydrogen combustion code validation measurements. This facility (Fig. 1), currently dedicated to scramjet-related experiments,[10,11] is designed to ultimately provide combustor entrance conditions simulating vehicle flight in the hypersonic window delimited by Mach numbers of 5.5 to 7.5 and altitudes of 15 to 55 km (Fig. 2).

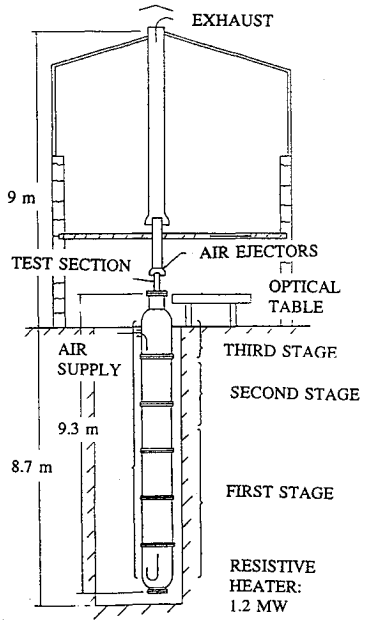

Fig. 1 Scramjet experimental facility.

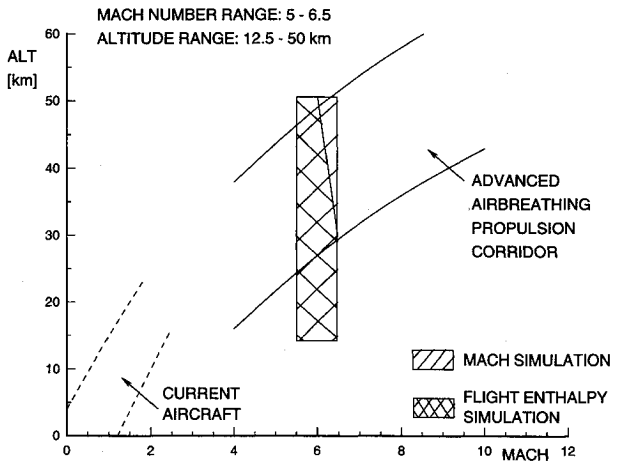

Fig. 2 Hypersonic flight simulation.

Staged installation of the heater provides increments in available total-air-temperature capability. In the current configuration heater modules provide outlet air temperatures to 1300 K. Sealing of the facility has included provision for operation to total air temperature of 2000 K with completion of design and addition of advanced heating modules. The oil-free compressor system provides continuous flows to 0.75 kg/s, sufficient for the operation of a 2.54- × 3.81-cm Mach 2 test section to 1-atm static pressure and air total temperatures above 660 K. A downstream air ejector permits the operation of a test section down to one-sixth atmosphere static pressure, encompassing anticipated inlet flight conditions for a supersonic combustor. The air is heated by an electric resistance (and, therefore, nonvitiating) heater. At present, a two-dimensional, water-cooled Laval nozzle, accelerates the air to Mach 2. A hydrogen heater will permit increasing the temperature of the fuel to 500 K prior to being injected in the combustor (not used in the experiments presented herein).

Test Section

Figure 3 shows a schematic diagram of the constant area test section used in these experiments. The air enters at Mach 2 and the fuel is injected normal to the flow and downstream of the 5-mm rearward-facing step at sonic conditions. The recirculation region formed behind the step is the main flameholding mechanism. Other flameholding mechanisms are provided by the recirculation regions in front of and between the jets. The test section was designed to offer good optical access to the flow to permit nonintrusive, laser-based measurements of the primitive variables. For the total temperature range of the current studies, operation with large, unshielded quartz windows placed on the three sides of the combustor using external silicone seals was possible for extended periods. At high stagnation temperatures the windows need to be shielded from the hot gases by a film of cool air. The length of the windows is limited by the effectiveness of the film shield. Several sets of combustor walls were designed, each one including windows at a different downstream location to permit the investigation of an entire flowfield. They also provide a geometric overlap that allows continuity of the experimental profiles. At low temperatures the side walls, such as those reported here, were replaced by full uncooled quartz windows that permitted complete optical access to the test section flowfield.

The length of the test section is 21.3 cm and the cross section is 2.5 by 3.8 cm. Along the injection wall pressure and temperature are measured to infer combustion efficiency. The fuel can be injected in various combinations from a set of nine injectors placed in three rows at 3, 7, and 12 step heights (5 mm step height) downstream of the step. The injectors can be fueled independently, with injector diameters of 1, 1.5, and 2.0 mm studied to date. Thermal choking limits the maximum hydrogen flow rates used.

Data Acquisition and Analysis

Tunnel operating conditions including critical heater temperatures were monitored by computer. One hundred twenty

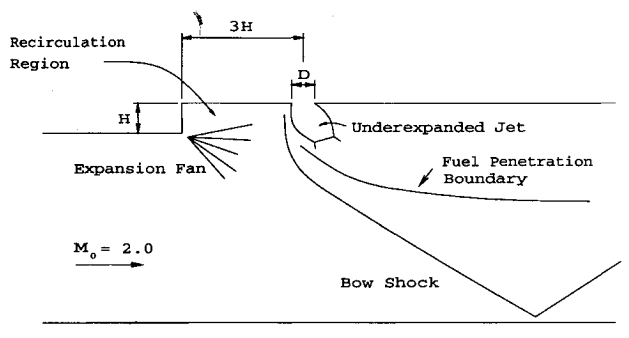

Fig. 3 Flowfield schematic.

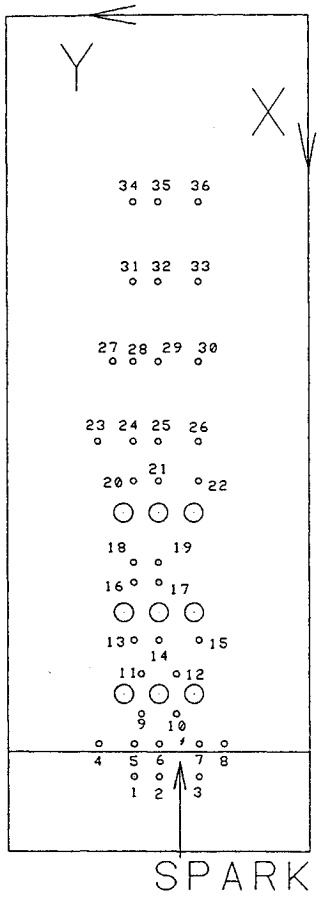

Port	X	Y
	cm	cm
1	19.4	3.8
2	19.4	3.8
3	19.4	4.4
4	18.6	5.3
5	18.6	4.4
6	18.6	3.8
7	18.6	2.8
8	18.6	2.1
9	17.8	4.2
10	17.8	3.4
11	16.8	4.2
12	16.8	3.4
13	16.0	4.4
14	16.0	3.8
15	16.0	2.8
16	14.5	4.4
17	14.5	3.8
18	14.0	4.4
19	14.0	3.8
20	11.9	4.4
21	11.9	3.8
22	11.9	2.8
23	10.9	5.3
24	10.9	4.4
25	10.9	3.8
26	10.9	2.8
27	8.8	5.0
28	8.8	4.4
29	8.8	3.8
30	8.8	2.8
31	6.8	4.4
32	6.8	3.8
33	6.8	2.8
34	4.8	4.4
35	4.8	3.8
36	4.8	2.8

Fig. 4 Wall instrumentation and fuel injectors.

channels of data were recorded with monitor display and periodic plotting of the most critical parameters.

Combustor wall pressures on the injection block were measured using a scanivalve™ model J interfaced to an EXV Entran Devices pressure transducer with valve controls and pressure recording by a second PC. A total of 36 wall pressure taps, with locations shown in Fig. 4, were recorded. Wall temperatures were also recorded with K-type thermocouples inserted 0.1 mm of the internal surface, placed in the base of the step, at the combustor midsection, and at the exit of the test section. The data acquisition was organized on three levels as follows:

1) On-line data display for test monitoring purposes: Each pressure tap was scanned for 1 s at a sampling rate of 5 samples/s. All five readings were displayed to assure equilibration, then averaged and stored. Following this, the valve was moved to the next pressure port. The procedure was repeated until all pressures were displayed and recorded.

2) Pressure distribution display: Immediately after all the wall-pressures were recorded the pressure distribution along the combustor was made available. Prior to being plotted, the wall pressures were normalized for small fluctuations (typically less than 0.5%) in the stagnation pressure.

3) Off-line (final) results: Typically, 2–5 min were required to iterate to a solution with a code used to predict streamwise parameters distribution from the operating parameters and measurements. The final output provided the combustion efficiency, the mixing efficiency, the axial temperature and velocity distribution, and gas composition.

The numerical algorithm, called generically combustion analysis (COMBAN[12]), was implemented, together with the data acquisition in a data acquisition and analysis system. This one-dimensional code makes use of measured wall pressure and temperature distribution for a given geometry, to compute Q_w, τ_w, and predict η_c distribution along with averaged values of the Mach number and species concentration. The chemical composition is calculated using a five-reaction model, while the turbulent mixing is calculated at each step based on η_m, defined as the amount of fuel that participates in the full reaction divided by the amount of fuel that would react if the mixture were uniform. This parameter is calculated based on empirical data obtained previously through extensive experiments.[12] η_c is calculated as the ratio between ϕ_r and ϕ_t:

$$\eta_c = (\phi_r/\phi_t) \tag{1}$$

This algorithm is clearly limited by the one-dimensional and equilibrium assumptions. Nevertheless, it is a useful tool in early parametrical studies, providing a solution in typically 2–5 min on a 286-based PC, thus enabling one to identify trends as various aerothermodynamic and geometrical parameters are changed. By comparison, detailed three-dimensional, time-accurate solutions require extensive CPU calculation on supercomputers.

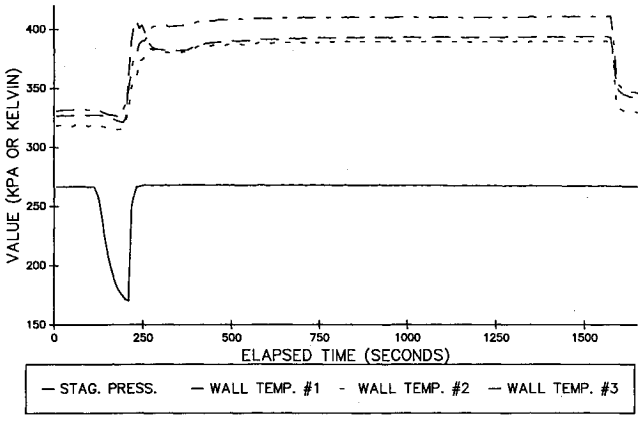

Fig. 5 Ignition sequence.

Ignition Procedure

At the relatively low stagnation temperatures of these experiments the ignition delay time for H_2-air reactions is typically longer than the residence time in the test section. To achieve ignition, the test section included a spark ignitor located in the base of the step and two adjacent pressure ports (6 and 7 in Fig. 4), which have been modified for use as hydrogen pilot injectors. Even so, with pilot injectors and spark operating, the Mach number in the region of the jet(s) is too large for fuel ignition. Therefore, the ignition sequence proceeded as shown in the time trace in Fig. 5. Initially, the pressure was reduced until the nozzle partially unstarted and the flowfield in the test section became subsonic. The hydrogen pilots and the main fuel injectors were then activated with the spark igniting the mixture in the recirculation zone. Then, the stagnation pressure was raised, and, when nominal operating stagnation pressure was achieved, the fuel pilots and the spark were turned off, and the supersonic combustion flow established. Final target stagnation pressure and temperature were then obtained with testing proceeding at steady-state fluid and boundary conditions for the duration of time required by the experiment (see Fig. 5).

Results

Thermal Choking

The combustor geometry for this investigation employed transverse sonic injection behind a rearward-facing step into a constant area duct. With this geometry and the low total temperature available ($T_0 < 800$ K), the combustor could only be operated at low overall equivalence ratios without incurring thermal choking and resultant upstream interaction. The

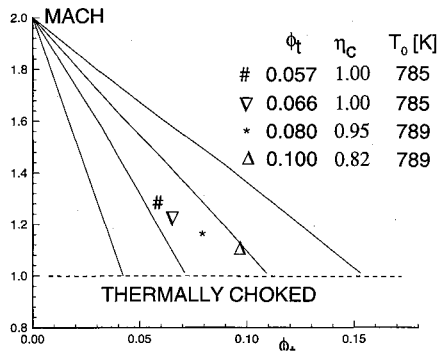

Fig. 6 Thermal choking.

conditions under which thermal choking occurs were predicted assuming complete combustion at the exit of the constant-area combustor. Experimental measurements indicated the extent of the applicability of this assumption.

Figure 6 shows the results of this analysis with the test section exit Mach number given as a function of ϕ_t for various main flow total temperature values. The overall equivalence ratio is defined as

$$\phi_t = \frac{(\dot{m}_{\text{fuel}}/\dot{m}_{\text{air}})_{\text{actual}}}{(\dot{m}_{\text{fuel}}/\dot{m}_{\text{air}})_{\text{stoich}}} \tag{2}$$

From this figure, the decrease in sensitivity of the Mach number to combustion heat release with increasing total temperature is evident. To avoid choking at higher equivalence ratios requires an increase in air total temperature or a divergent test section. At higher initial temperatures the Mach number is less sensitive to heat release, while a divergent section will counter the effect of heat release by acceleration of the supersonic flow.

The experimentally determined Mach numbers at the exit of the duct (obtained from wall pressure measurements and a one-dimensional prediction of combustion efficiency) agreed well with the theoretical thermal choking model, as shown by the experimental points in Fig. 6. For the cases in which a low mass flow of hydrogen was injected, the combustion was essentially complete. Here, the agreement between the experimental and calculated Mach numbers on Fig. 6 was good. As additional hydrogen was injected, the fuel was not as efficiently mixed with the freestream air and the combustion efficiency dropped. Thus, the experimental conditions at which thermal choking was encountered tended toward a higher ϕ_t than predicted from the complete combustion calculation.

Pressure Distribution in the Duct

Figure 7 shows a typical measured pressure distribution in the duct without injection and with injection and combustion, as noted in the figure. Measured pressure distribution with fuel flow and no combustion was essentially identical to those with no fuel flow at the low fueling rates of these studies. Following measurement, the averaged pressure at each axial location was normalized to the combustor entrance conditions.

For the rearward-facing step geometry, in the absence of fuel injection, the flow expands behind the step and the static pressure drops in the base to about 45% of the inlet value. The pressure recovers further downstream as the flow is compressed after reattachment on the wall. The expansion fan intersects the injection wall downstream after reflecting from the opposite wall, producing a gradual decrease in pressure approximately 10 step heights from the step. The shock generated at the reattachment also reflects from the opposite wall and produces the sharp pressure rise at approximately 25 step heights downstream from the step. These features can be noted in the pressure distribution obtained with injection, but without combustion.

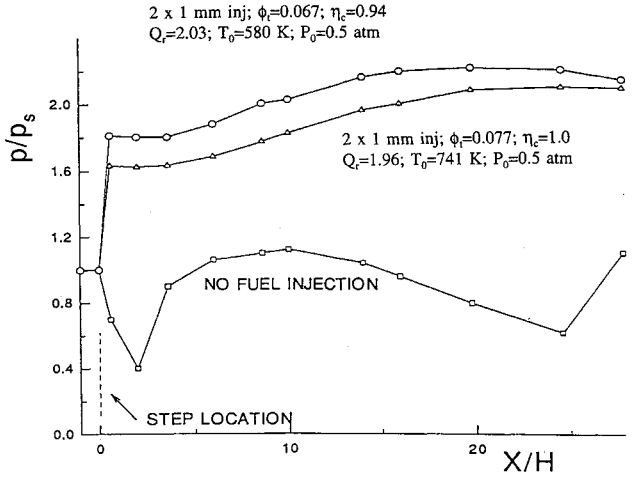

Fig. 7 Wall-averaged pressure distribution.

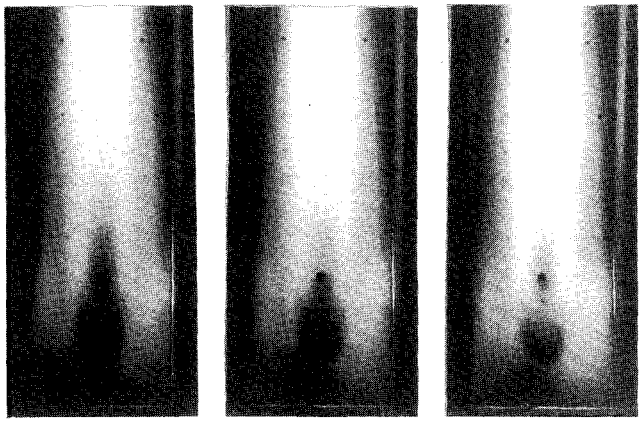

Fig. 8 Effect of air total temperature: water vapor emission photograph.

With combustion, fuel is trapped in the recirculation zone where it burns, creating a region of hot gases and providing the main flameholding mechanism. At the low equivalence ratios of these tests, most of the combustion occurred in the recirculation zone and around the jet. As a result, most of the pressure rise (about 70%) is experienced immediately behind the step (see Fig. 7). The pressure upstream of the step is shown to be unaffected by the combustion, which indicates that the step provides good isolation between the combustor and the upstream supersonic flow despite the large jump in downstream pressure.

At the lower air stagnation temperature the pressure increase is greater than at the higher temperature; however, this is accompanied by a decrease in the combustion efficiency. The explanation of this behavior with air stagnation temperature is discussed in the following sections.

Coupled Effect of Air Total Temperature and Injection Dynamic Pressure Ratio

During the experiments it was observed that the flame produced a visible, pale blue emission.[13] Spectral scans of the emission were used to determine that the emission was due to chemiluminescence from both OH and H_2O. The visible portion was determined to result from H_2O (by comparison with a dispersion spectrum of two-photon dissociation of H_2O).[14] Consequently, flame visualization photographs using the visible H_2O emission were obtained through a window viewing the injection wall.

Figure 8 shows several H_2O emission photographs obtained. In these photographs the main flow is from bottom to top and the fuel is injected in staged injection at $3H$ and $7H$, respectively, and is directed toward the observer. The

injector at $7H$ can be noted by the dark circle in the center of the duct. Due to the absence of flame emission in the region of the jet at $3H$, its position is not evident in the photographs. Three stagnation temperatures are represented: 741, 685, and 581 K, respectively. The injection dynamic pressure ratio, defined as

$$Q_r = \frac{(\gamma P_s M^2)_{\text{injector exit}}}{(\gamma P_s M^2)_{\text{air freestream}}} \tag{3}$$

was kept constant for the tests (the jet penetration is proportional to the dynamic pressure ratio in nonreacting flows). The equivalence ratio increased as the square root of the air total temperature (the injector area, total pressures of main flow and injector, and fuel total temperature were fixed). At higher initial total temperature a larger dark region relative to the lower temperature case is noted in the base of the step and between the jets. This is felt to be an indication of locally richer mixture and, consequently, fewer reactions are completed in this region, rather than a difference in chemical kinetics that would result in the reverse trend. A discussion of the mixing-combustion interaction in this flowfield follows, based on the Damköhler number for water formation.

The rate-limiting factor in this flowfield may be either mixing or combustion, depending on the axial position. At large Damköhler numbers (the ratio of fuel mixing to chemical reaction times), chemical reactions occur rapidly and the flow is mixing limited. For long chemical reaction times, the Damköhler number may drop below unity and combustion becomes the limiting factor. In particular, due to the high temperature and low velocity in the flame region surrounding the jet, the residence time of a fluid volume τ_f may be comparable to the chemical time, defined as the sum of τ_{ig}, and τ_r (the ignition delay time is defined as time corresponding to 5% of the adiabatic flame temperature rise, and the reaction time corresponds to the time for 5–95% of the adiabatic temperature rise). To estimate the order of the residence, ignition delay, and reaction times the results of a numerical simulation were used.[15] This estimation should provide typical parameters for this combustor. The residence time is calculated based on the jet penetration height (approximately $1.8H$), and an average velocity across the shear layer formed downstream of the jet plume of 180 m/s and is on the order of 50 μs. The ignition delay time for a pressure of approximately 1 atm and a temperature of about 2000 K ranges between 4–6 μs, and the reaction time between 8–10 μs. Thus, for this case, the Damköhler number approaches unity and the mixing and combustion time scales become comparable. In other regions of the flow, one of the two effects may become prevalent, although even under mixing limited conditions, mixing is affected by the heat release of combustion and the effects cannot be uncoupled.

As the dynamic pressure ratio increases, penetration and, therefore, mixing are improved. Simultaneously, the combustion increases the local pressure and reduces the local Mach number, and this, in turn, affects the mixing. The effect of heat release on the static pressure distribution (e.g., in Fig. 7), is obvious, although the dynamic pressure ratio is unchanged. Figure 9 presents the averaged cross section distribution of the Mach number estimated for the same experiments, and shows how the heat release has affected the streamwise Mach number distribution. It is, therefore, useful to introduce a new parameter to describe mixing and penetration in the presence of combustion, an "effective" injection dynamic pressure ratio, defined as

$$Q_r^{\text{eff}} = \frac{(\gamma P_s M^2)_{\text{injector exit}}}{(\gamma P_s M^2)_{\text{combustion freestream}}} \tag{4}$$

where the freestream dynamic pressure is now taken as representative of the conditions (i.e., p_s and M) with combustion.

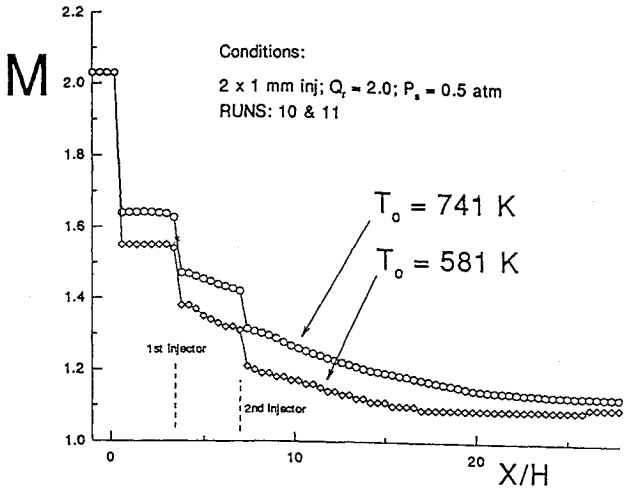

Fig. 9 Effect of air total temperature: Mach number distribution.

For the two sets of combustion measurements in Fig. 7, the local pressures (in the vicinity of the jet) change from 170 to 190% (of the inlet static pressure) for inlet temperatures of 741 and 581 K, respectively, while the Mach numbers decrease to 1.31 and 1.18, respectively. As a result of combustion the effective injection dynamic pressure ratio becomes

$$Q_r^{\text{eff}} = Q_r \frac{(\gamma P_s M^2)_{\text{injector exit}}}{(\gamma P_s M^2)_{\text{combustor freestream}}}$$

$$= Q_r \bar{p} \bar{M}^2 = Q_r \frac{1}{1.7} \frac{2^2}{1.31^2} = 1.37 Q_r \tag{5}$$

for $T_0 = 741$ K and

$$Q_r^{\text{eff}} = Q_r \frac{1}{1.9} \frac{2^2}{1.18^2} = 1.51 Q_r \tag{6}$$

for $T_0 = 541$ K. Thus, the penetration and mixing may be improved by the effect of heat release on the local fluid parameters responsible for mixing. It is proposed, therefore, that penetration and mixing in the presence of combustion should scale with Q_r^{eff}, not Q_r. The mixing will, therefore, increase as the air T_0 is decreased, due to an increase in Q_r^{eff}, which is in turn due primarily to a decrease in combustor Mach number as heat is added and thermal choking is approached. This explanation is consistent with the pressure rise in Fig. 7, which is greater for lower T_0 condition.

Figure 10 presents the calculated combustion efficiencies for air total temperatures of 581 and 741 K. A brief note on the algorithm currently implemented in the one-dimensional analysis is needed to explain the "abnormal" behavior of the curves in Fig. 10. Since COMBAN employs a downstream-marching calculation, no fuel is found in the code upstream of the injection station. The combustion efficiency is defined as the amount of fuel reacted divided by the amount of fuel injected. To avoid numerical overflow the code automatically sets the combustion efficiency to zero in regions upstream of the injection station. To match the actual upstream pressure rise, the code assumes a separation region. Figure 10 is a plot of the calculated combustion efficiency for staged injection using 1-mm injectors at both locations ($3H$ and $7H$, respectively). The present combustion efficiency code matches the pressure rise to the pressure increase due to the complete combustion of a certain amount of fuel in a given geometry. Upstream of the jets and between the jets the measured pressure rise is due to the effect of combustion of fuel from both injectors, which contribute equally to the total equivalence ratio. However, the code cannot account for fuel injection from the second jet before it actually reaches that spatial

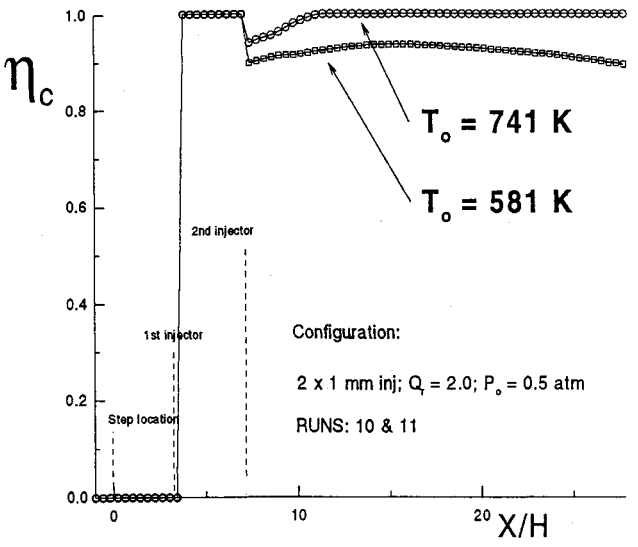

Fig. 10 Effect of air total temperature: combustion efficiency.

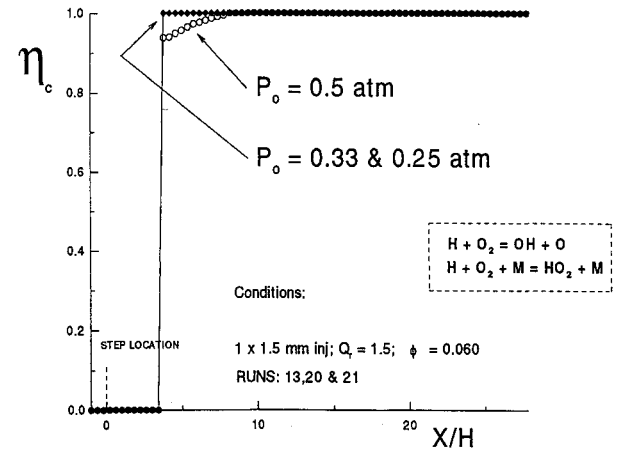

Fig. 11 Effect of air static pressure: single injector.

coordinate. Therefore, between the jets, the pressure rise during the experiment is larger than can be attributed to the contribution of the first jet only, and the calculated combustion efficiency reaches a limiting value of 100%. The additional pressure rise is interpreted by the code as a flow separation. Downstream of the location of the second jet, the code matches the pressure measured during the experiment to a pressure rise resulting from combustion of fuel injected from both injectors and, therefore, the combustion efficiency decreases (see Fig. 10). The combustion efficiency should be calculated correctly (under the approximations of one dimensionality and chemical equilibrium) downstream of the second jet. In short, the combustion efficiency distribution along a given combustor, prior to injection of the entire mass of fuel is only a qualitative indication of combustion behavior. As an "absolute" quantitative value of combustion efficiency for a given geometry/fuel injection configuration, the integrated value at the exit of the domain should be used.

The following two statements summarize the coupled effect of fluid dynamics and chemical kinetics described in this section:

1) At lower air total temperatures the "effective" injection dynamic pressure ratio is increased, producing better penetration and mixing, and producing a larger pressure rise in the flameholding region in the base of the step (see Fig. 7).

2) The reduction in air total temperature should increase the chemical reaction time, and results in a lower overall combustion efficiency for a fixed combustor length. This is consistent with the results in Fig. 10.

Effect of Air Static Pressure

At temperatures typical of the present experiments, approximately 800 K, τ_{ig} is controlled by the competition between the bimolecular chain-branching reaction

$$H + O_2 = OH + O \tag{7}$$

and the trimolecular chain-terminating reaction

$$H + O_2 + M = HO_2 + M \tag{8}$$

As the pressure is reduced and the second explosion limit is approached (the boundary that separates the regions of slow and fast reaction at low pressures and temperatures for H_2-air reaction), the probability of the three-body collision is reduced and the balance shifts toward the chain-branching reaction. This reduces the ignition delay time and results in more rapid reactions. The effect of pressure on τ_r was found to be less substantial than on the ignition delay time.[16] The resulting change in the ignition delay time is large enough compared to the gas residence time to allow the kinetics to affect the flowfield.

The present experimentally derived combustion efficiency is consistent with this theoretically predicted effect of pressure. In Fig. 11, it is seen that as the air static pressure is reduced from 0.5 to 0.33 and 0.25 atm, the combustion takes place more rapidly, and essentially all the fuel reacts in the vicinity of the jet. A similar behavior was noted for staged injection. Therefore, it is concluded that reducing the air static pressure improves the combustion efficiency by decreasing the ignition delay time.

Conclusions

An experimental study of a scramjet model at low stagnation temperatures and low equivalence ratios was conducted. Parametric investigation of the effects of initial conditions was reported. From this, the following has been concluded:

1) The combination of a constant area duct and low combustor entrance temperatures results in high efficiency and upstream interaction at low equivalence ratios (ϕ_r = 0.1 in this case). As the equivalence ratio is increased and the rate of heat release is reduced (i.e., lower combustion efficiency), thermal choking is being delayed.

2) Neither autoignition nor spark ignition was achieved at the current stagnation temperatures levels in supersonic flow. However, following ignition with an external source and removal of this source, the combustion is self-sustained to total temperatures as low as 300 K.

3) The pressure increase associated with combustion reduces the three dimensionality of the flow. The typical pressure variation in a crossflow section in regions up and downstream of the jets does not exceed 10%. Clearly, this is not true for the immediate region of the barrel shock around the underexpanded jet in which no detailed measurements were obtained.

4) Due to large gradients in the flowfield of this combustor there are regions in which either mixing or chemical reactions rates will control the combustion. Typical conditions in the region of the jets can be characterized by a Damköhler number of $\mathcal{O}(1)$. Thus, it may be expected that neither mixing nor reaction rates will dominate in this region. Use of initial conditions to scale fuel mixing does not include the flowfield properties when combustion is present. A more appropriate description of the combustor conditions in the vicinity of the jet may be provided through an effective dynamic pressure ratio that includes the effects of combustion on the local flow conditions used to scale penetration and mixing.

Acknowledgments

This work was sponsored by NASA Langley Research Center, Hampton, Virginia, Grant NAG-1-795, G. Burton Northam, Technical Monitor.

References

[1]Dimotakis, P., "Turbulent Free Shear Layer Mixing," AIAA Paper 89-0262, June 1989.

[2]Samimy, M., Erwin, D. E., and Elliot, G. S., "Compressibility and Shock Wave Interaction Effects on Free Shear Layer," AIAA Paper 89-2460, July 1989.

[3]Papamoschou, D., and Roshko, A., "Observations of Supersonic Free Shear Layers," AIAA Paper 86-0162, Jan. 1986.

[4]Barlow, R. S., Fourguette, D. C., Mungal, M. G., and Dibble, R. W., "Structure of a Supersonic Reacting Jet," AIAA Paper 91-0376, Jan. 1991.

[5]Hermanson, J. C., and Dimotakis, P. E., *Journal of Fluid Mechanics*, No. 199, 1989, pp. 513–553.

[6]Northam, G. B., Greenberg, I., and Byington, C. S., "Evaluation of Parallel Injector Configurations for Supersonic Combustion," AIAA Paper 89-2525, July 1989.

[7]Capriotti, D. P., Northam, G. B., Greenberg, I., and Byington, C. S., "Evaluation of Parallel Injector Configurations for a Mach 3 Combustor," 26th JANNAF Combustion Meeting, Pasadena, CA, Oct. 1989.

[8]Brescianini, C. P., and Morgan, R. G., "An Investigation of a Wall-Injected Scramjet Using a Shock Tunnel," AIAA Paper 92-3965, July 1992.

[9]Rogers, R. C., and Schexnayder, C. J., "Chemical Kinetic Analysis of Hydrogen-Air Ignition and Reaction Times," NASA TP 1856, July 1981.

[10]Krauss, R. H., McDaniel, J. C., Scott, J. E., Jr., Whitehurst, B. R., Segal, C., Mahoney, G. T., and Childers, J. M., "Unique, Clean-Air, Continuous Flow, High-Stagnation-Temperature Facility for Supersonic Combustion Research," AIAA Paper 88-3059, July 1988.

[11]Krauss, R. H., Segal, C., Abbitt, J. D., Whitehurst, B. R., and McDaniel, J. C., "Initial Supersonic Combustion Facility Measurements," AIAA Paper 89-2462, July 1989.

[12]Diskin, G. S., and Northam, G. B., "Effects of Scale on Supersonic Combustion," AIAA Paper 87-2164, June 1987.

[13]Abbitt, J. D., III, Segal, C., McDaniel, J. C., Krauss, R. H., and Whitehurst, R. B., "Experimental Supersonic Hydrogen Combustion Employing Staged Injection Behind a Rearward-Facing Step," *Journal of Propulsion and Power*, Vol. 9, No. 3, 1993, pp. 472–478.

[14]Engel, V., Meijer, G., Bath, A., Anderson, P., and Schinke, R., "The C → A Emission in Water: Theory and Experiment," *Journal of Chemical Physics*, Vol. 87, No. 8, 1987, pp. 4310–4314.

[15]Segal, C., Haj-Hariri, H., and McDaniel, J. C., "A Numerical Investigation of Hydrogen Combustion in a Mach 2 Airflow," AIAA Paper 92-0341, Jan. 1992.

[16]Hitch, B. D., and Senser, D. W., "Reduced H_2-O_2 Mechanisms for Use in Reacting Flows," AIAA Paper 88-0732, Jan. 1988.